Fixed-Gain Augmented-State Tracking-Filters

Hugh L. Kennedy
NSI Division, DST Group
Edinburgh, Adelaide, Australia
Hugh.Kennedy@dst.defence.gov.au

***Abstract*—The complex frequency response is a complete description of a tracking filter's behavior at steady state. For example: 1) The flatness order at zero frequency determines the kinematic state dimension, thus the polynomial degree of trackable target trajectories; 2) The magnitude and phase error at a given non-zero frequency determine the radial and angular (bias) errors for a target on a circular orbit of a given angular velocity; and 3) The integral of squared magnitude determines the (random) measurement-noise attenuation. A procedure for the design of fixed-gain tracking filters, using an augmented-state observer with signal and interference subspaces, is proposed as a way of satisfying these frequency-response requirements. The signal subspace incorporates an integrating Newtonian model and a second-order maneuver model that is matched to a sustained constant-g turn; the deterministic interference model attenuates high frequencies for smoother track estimates. The selected models provide a simple means of shaping the steady-state response of tracking-filters of elevated order, when noise statistics are unknown and non-Gaussian. Pole placement is used to tune the transient response as an alternative to process noise.**

Keywords— IIR filters, Kalman filters, Noise shaping, Observers, State estimation, Tracking loops

I. INTRODUCTION

The exploitation of prior knowledge by the Kalman filter (KF) gives rise to a variable gain and adaptive behavior, which is highly desirable in automatic target-tracking systems. Knowing the parameters of (Gaussian) measurement-noise and process-noise statistics, and the covariance of the state estimate that follows, provides additional leverage that may be used to: accelerate the removal of bias errors during track establishment; handle changing sensor/target characteristics; accommodate variable revisit intervals; and manage measurement-to-track assignment ambiguities that arise in the presence of clutter, multiple closely-spaced targets, and missing measurements.

For measurement statistics, the use of a Gaussian prior is usually a reasonable approximation; however, for process statistics it may be unreasonable, particularly for agile targets that execute rare, extreme, and diverse, maneuvers. When noise parameters are unknown and very non-Gaussian, maintaining the covariance matrix and evaluating the resulting filter gain on each update is an expensive overhead that does not necessarily improve tracking accuracy [1]. In these cases, fixed-gain filters that do not incorporate prior knowledge of second-order statistical moments, i.e. the variance of noise distributions, are more appropriate. The resulting filter structures make it easier to incorporate more detailed process models that would otherwise be difficult to parameterize, analyze, and realize, within a stochastic framework.

A popular way of designing basic fixed-gain filters begins with a KF for position-velocity(-acceleration) states; the steady-state (SS) Kalman gain vector is then determined via the Riccati equations. For a SS-KF of order K, with noise matrices $\boldsymbol{Q}$ and $\boldsymbol{R}$ of a specified form, this method yields closed-form expressions for $\alpha - \beta$ ($K = 2$) or $\alpha - \beta - \gamma$ ($K = 3$) filter coefficients, as a function of the dimensionless $\lambda_{\mathrm{SS-KF}} = T_s^2\sigma_Q/\sigma_R$ quantity, which combines the sampling period T_s and noise parameters, where σ_Q & σ_R are the standard deviations of the process-noise and measurement-noise distributions, respectively [1]. This parameter is commonly referred to as the tracking index [2]. General procedures for integrating models of arbitrary order, for a wider filter bandwidth, are available [1],[3]; however, this is likely to degrade tracking performance without additional measures to attenuate noise and interference.

An alternative class of methods begins by specifying some aspect of the transient response and/or the SS response (e.g. signal bandwidth or noise gain), then proceeds with the discrete-time transfer-function/frequency-response of the tracking filter as the design object, rather than a set of assumed statistical distributions [4]-[13]. From these requirements, the $\alpha - \beta(-\gamma)$ parameters of a fixed-gain filter [5]-[11], or the process-noise parameter of a variable-gain KF are then derived [12],[13].

The merit of using deterministic analysis to design stochastic (i.e. Kalman) filters is questioned in [9] and the possibility of using state observers (e.g. Luenberger) with arbitrarily placed poles, is mooted; however, details of how such a design procedure might be adapted for this specific purpose are not provided. Posing the tracking problem in the transform domain (i.e. z or ω) simplifies the algebraic manipulations required to derive tracking filter coefficients [14],[15] and performance metrics [11]. It also opens the door to other design and analysis possibilities that have not hitherto been utilized in target-tracking problems.

Discrete-time shaping-filters with augmented states and a variable gain were originally formulated for handling colored noise in communications systems [16],[17]; they have since been extended to incorporate online system identification and applied to a variety of problems, such as speech processing [18]-[20]. In this paper, a steady-state variant is used to solve the Newtonian target-tracking problem: A deterministic process model – with signal and interference subspaces – and without random-noise terms is utilized, to provide a way of balancing conflicting bandwidth/noise-gain requirements in a filter of elevated order.

Unlike conventional methodologies described in the literature, that are based on the parameters of random process-and measurement-noise statistics, the tracker design and analysis procedure presented in this paper revolves around the tracking filter's frequency response. It is shown that deterministic process models may be crafted to shape the response, for improved maneuver handling at specified rates of turn and/or increased track smoothness at steady state. Pole-placement – standard in controller design but unusual in tracker design – is then used to determine the convergence behavior after track initiation and input discontinuities (e.g. steps or ramps), i.e. the transient response. The frequency response of the tracking filter determines its behavior at steady-state, whereas the position of the (repeated and real) poles determines its behavior as it approaches steady-state.

The problem of tracking a point target in a Cartesian coordinate system is considered here – a distant target in a high-resolution imaging radar, for example. Target and measurement dynamics are assumed to be approximately linear over the spatial and temporal scales of the sensor and the states are assumed to be independent and separable in both Cartesian dimensions. The derivation that follows, deals with a single scalar measurement from one of the dimensions and measurement-to-track assignment is unambiguous. Extensions that incorporate data association will be described in a future publication. A constant time interval (T_s) between measurements is also assumed.

II. Formulation

The sequence of measurements collected by the sensor is assumed to be generated by an endogenous linear-time-invariant (LTI) process with signal and interference subspaces. The signal subspace is further assumed to contain target and maneuver terms. The target model governs baseline dynamics; it is an integrating process, with K_{tgt} repeated poles at the origin of the complex s-plane. This basic Newtonian process may be augmented to include a complex conjugate pair of poles on the imaginary axis, near the origin, to model a low-frequency sinusoidal oscillation (i.e. a weave maneuver [4]), or a circular orbit (i.e. a sustained constant-g turn) in two Cartesian dimensions. Similar considerations have been used elsewhere to determine the bandwidth requirements for $\alpha-\beta(-\gamma)$ filters [10],[11]; however, explicitly including this term in the process model eliminates SS position-tracking errors, for a perfectly matched maneuver. An interference model may also be included to remove unwanted high-frequency noise, or simply for the aesthetic of smoother tracks.

This fully deterministic formulation greatly simplifies the filter derivation and realization because the Riccati equations and covariance matrix manipulations are not required; moreover, despite the omission of explicit random-noise terms, the resulting fixed-gain filters confer excellent noise suppression via the interference model.

The "process" is a continuous-time natural system; whereas the "observer" is a discrete-time synthetic system, employing a model of the natural system, which is realized on a digital computer. The two systems are connected via a one-way flow of sampled sensor measurements. Feedback exists within both systems but feedback between the two systems is not considered here. The observer seeks to estimate the hidden states of the process. In this section it is assumed that the process model is perfect; the impact of modelling errors is discussed in the section that follows.

A. Target process model

The linear state-space (LSS) representation, of this continuous-time process, in controller-canonical form (CCF), is as follows:

$\dot{\boldsymbol{w}}_{\text{tgt}}(t) = \boldsymbol{A}_{\text{tgt}}\boldsymbol{w}_{\text{tgt}}(t)$, $y_{\text{tgt}}(t) = \boldsymbol{C}_{\text{tgt}}\boldsymbol{w}_{\text{tgt}}(t)$ with

$$\boldsymbol{A}_{\text{tgt}} = \begin{bmatrix} \boldsymbol{0}_{(K_{\text{tgt}}-1)\times 1} & \boldsymbol{I}_{(K_{\text{tgt}}-1)} \\ 0 & \boldsymbol{0}_{1\times(K_{\text{tgt}}-1)} \end{bmatrix}_{K_{\text{tgt}}\times K_{\text{tgt}}} \text{ and}$$

$$\boldsymbol{C}_{\text{tgt}} = \begin{bmatrix} 1 & \boldsymbol{0}_{1\times(K_{\text{tgt}}-1)} \end{bmatrix}_{1\times K_{\text{tgt}}} \tag{1}$$

where $y_{\text{tgt}}(t)$ and $\boldsymbol{w}_{\text{tgt}}(t)$ are the output signal and the process states; furthermore, $\boldsymbol{I}_N$ is an $N\times N$ identity matrix and $\boldsymbol{0}_{M\times N}$ is an $M\times N$ matrix of zeros; thus $\boldsymbol{A}_{\text{tgt}}$ is a zero matrix with ones along the 1st upper diagonal. The corresponding discrete-time model, for a constant sampling period of T_s, is found via the s domain in the usual way [21],[22], using

$$\boldsymbol{G}_{\text{tgt}} = \mathcal{L}^{-1}\{\boldsymbol{\Phi}_{\text{tgt}}(s)\}\big|_{t=T_s} \text{ where} \tag{2a}$$

$$\boldsymbol{\Phi}_{\text{tgt}}(s) = \left(s\boldsymbol{I}_{K_{\text{tgt}}} - \boldsymbol{A}_{\text{tgt}}\right)^{-1} \text{and} \tag{2b}$$

$\mathcal{L}^{-1}$ is the inverse Laplace transform ($t \leftarrow s$). The state-transition matrix $\boldsymbol{G}_{\text{tgt}}$, is an upper-triangular Toeplitz matrix with the elements along the kth off-diagonal (for $k = 0 \ldots K_{\text{tgt}}-1$) equal to $\mathcal{G}(k;T_s) = T_s^k/k!$. As the diagonal elements of this triangular matrix are equal to unity, the discrete-time model of the target signal has K_{tgt} repeated poles in the complex z-plane at $z=1$, for a singularity at dc, i.e. at $\omega = 0$, where ω is the angular frequency (radians per sample).

B. Maneuver process model

This second-order term is defined in CCF as follows:

$\dot{\boldsymbol{w}}_{\text{man}}(t) = \boldsymbol{A}_{\text{man}}\boldsymbol{w}_{\text{man}}(t)$, $y_{\text{man}}(t) = \boldsymbol{C}_{\text{man}}\boldsymbol{w}_{\text{man}}(t)$ with

$$\boldsymbol{A}_{\text{man}} = \begin{bmatrix} 0 & 1 \\ -\Omega^2 & 0 \end{bmatrix} \text{ and } \boldsymbol{C}_{\text{man}} = \begin{bmatrix} 1 & 0 \end{bmatrix} \tag{3a}$$

where Ω is the angular velocity (rad/s), or maneuver turn rate, for a constant-speed orbit of radius R; thus

$$\boldsymbol{G}_{\text{man}} = \begin{bmatrix} \cos(\Omega T_s) & \sin(\Omega T_s)/\Omega \\ -\Omega\sin(\Omega T_s) & \cos(\Omega T_s) \end{bmatrix} \tag{3b}$$

which has poles in the z-plane at $z = e^{\pm i\Omega T_s}$ where $i^2 = -1$. Note that $\boldsymbol{A}_{\text{man}}$ and $\boldsymbol{G}_{\text{man}}$ are for the continuous-time and discrete-time processes, respectively. The latter representation is derived from the former via the same standard procedure used to discretize the target process model in (2).

A second-order *damped* oscillator is used in [23] to model "wind sway or platform roll". It is an extension of the Singer model, which shifts a pole at the origin of the s-plane, left along the real axis [15],[24]. Although, this result is derived via the introduction of first-order auto-correlation in the noise input, its effect may be physically interpreted as a drag force acting on the target, for a second-order process, with position and velocity states, an acceleration input and a position output.

The *undamped* one-dimensional (1-D) oscillator used here in (3a), with poles on the imaginary axis of the s-plane at $\pm\Omega$, may seem somewhat unrealistic for a target's motion in 1-D; however, when two such models are placed in parallel, to represent independent motion in two orthogonal Cartesian axes, they may be used to perfectly model circular motion, when their internal states fall into antiphase. Unlike the 2-D coordinated turn models discussed in [25], the relative phase and magnitude of these parallel maneuver state-estimates in the observers that follow, are unconstrained and free to drift in a way that best accounts for the input data sequence; thus additional maneuver detection and model switching or mixing is not required. In addition to reducing computational complexity, this simplification allows linear–systems theory to be used for the design and analysis of the fixed-gain tracking filters that result. The cost of the proposed maneuver model is an increase in the measurement-noise gain, particularly if fast and tight turns are accommodated; however, this is partially offset by the interference process model.

C. *Interference process model*

Proceeding along similar lines, the interference process is a K_{int}th-order system with K_{int} repeated poles at $z = -1$, for a singularity at $\omega = \pi$. In this case $\boldsymbol{G}_{\mathrm{int}}$, which has the same Toeplitz structure as $\boldsymbol{G}_{\mathrm{tgt}}$, is populated using $-\mathcal{G}(k; T_s)$ for $k = 0 \ldots K_{\mathrm{int}} - 1$, thus $\boldsymbol{G}_{\mathrm{int}} = -\boldsymbol{G}_{\mathrm{tgt}}$ and $\boldsymbol{C}_{\mathrm{int}} = \boldsymbol{C}_{\mathrm{tgt}}$ when $K_{\mathrm{int}} = K_{\mathrm{tgt}}$.

The form of this model is not physically motivated; rather, it is adopted to attenuate very high-frequency noise, which is assumed to be particularly undesirable, from sources inside or outside the sensor. An interferer of any frequency may in principle be defined; however, using an oscillation frequency of π allows real poles to be used, instead of complex conjugate pairs, for a lower filter order. Using a frequency at the extremum of the spectrum also minimizes distortion in the signal band near dc. A single pole is generally sufficient for this model; however, degenerate poles may be used to extend its influence to lower frequencies, for a wider stopband.

D. *Process model*

The discrete-time model of the process that generates the sampled measurement sequence (i.e. "the process") may now be defined as

$\boldsymbol{w}_{\mathrm{prc}}(n) = \boldsymbol{G}_{\mathrm{prc}}\boldsymbol{w}_{\mathrm{prc}}(n-1)$ and

$y_{\mathrm{prc}}(n) = \boldsymbol{C}_{\mathrm{prc}}\boldsymbol{w}_{\mathrm{prc}}(n)$ where

$$\boldsymbol{w}_{\mathrm{prc}}(n) = \begin{bmatrix} \boldsymbol{w}_{\mathrm{tgt}}(n) \\ \boldsymbol{w}_{\mathrm{man}}(n) \\ \boldsymbol{w}_{\mathrm{int}}(n) \end{bmatrix}_{K\times 1}$$

$$\boldsymbol{G}_{\mathrm{prc}} = \begin{bmatrix} \boldsymbol{G}_{\mathrm{tgt}} & \boldsymbol{0}_{K_{\mathrm{tgt}}\times K_{\mathrm{man}}} & \boldsymbol{0}_{K_{\mathrm{tgt}}\times K_{\mathrm{int}}} \\ \boldsymbol{0}_{K_{\mathrm{man}}\times K_{\mathrm{tgt}}} & \boldsymbol{G}_{\mathrm{man}} & \boldsymbol{0}_{K_{\mathrm{man}}\times K_{\mathrm{int}}} \\ \boldsymbol{0}_{K_{\mathrm{int}}\times K_{\mathrm{tgt}}} & \boldsymbol{0}_{K_{\mathrm{int}}\times K_{\mathrm{man}}} & \boldsymbol{G}_{\mathrm{int}} \end{bmatrix}_{K\times K}$$

$\boldsymbol{C}_{\mathrm{prc}} = [\boldsymbol{C}_{\mathrm{tgt}} \quad \boldsymbol{C}_{\mathrm{man}} \quad \boldsymbol{C}_{\mathrm{int}}]_{1\times K}$ and

$K = K_{\mathrm{tgt}} + 2K_{\mathrm{man}} + K_{\mathrm{int}}$, with $K_{\mathrm{man}} \le 1$

($[\cdot]^T$ is the transpose operator). (4)

Note that the signal and interference models used here are just examples of possible processes that may be relevant in a tracking problem. Other process definitions and permutations are possible; however, this particular combination was found to provide sufficient flexibility and control over tracking behavior in typical problems.

E. *Observer design*

As the process has K poles on the unit circle, it is marginally stable. We now seek a stable observer, i.e. all poles inside the unit circle, to estimate the states of the augmented-state vector, placed in series with the process, that has the following discrete-time LSS representation:

$\hat{\boldsymbol{w}}_{\mathrm{prc}}(n) = \boldsymbol{G}_{\mathrm{prc}}\hat{\boldsymbol{w}}_{\mathrm{prc}}(n-1) + \boldsymbol{\mathcal{K}}\{x(n) - \hat{x}(n)\}$ or

$\boldsymbol{w}_{\mathrm{obs}}(n) = \boldsymbol{G}_{\mathrm{obs}}\boldsymbol{w}_{\mathrm{obs}}(n-1) + \boldsymbol{H}_{\mathrm{obs}}x(n)$ and

$y(n) = \boldsymbol{C}_{\mathrm{obs}}\boldsymbol{w}_{\mathrm{obs}}(n)$ where: (5a)

$y(n)$ is the smoothed output of the observer

$\boldsymbol{C}_{\mathrm{obs}} = [\boldsymbol{C}_{\mathrm{tgt}}\boldsymbol{G}_{\mathrm{tgt}}(q) \quad \boldsymbol{C}_{\mathrm{man}}\boldsymbol{G}_{\mathrm{man}}(q) \quad \boldsymbol{0}_{1\times K_{\mathrm{int}}}]_{1\times K}$

$\boldsymbol{w}_{\mathrm{obs}} = \hat{\boldsymbol{w}}_{\mathrm{prc}}$, $\boldsymbol{H}_{\mathrm{obs}} = \boldsymbol{\mathcal{K}}$, $\boldsymbol{G}_{\mathrm{obs}} = \boldsymbol{G}_{\mathrm{prc}} - \boldsymbol{\mathcal{K}}\boldsymbol{C}_{\mathrm{prd}}$

$\boldsymbol{C}_{\mathrm{prd}} = \boldsymbol{C}_{\mathrm{prc}}\boldsymbol{G}_{\mathrm{prc}}$ (i.e. a one-step-ahead predictor)

$\hat{\boldsymbol{w}}_{\mathrm{prc}}(n)$ is the estimate of $\boldsymbol{w}_{\mathrm{prc}}(n)$

$\boldsymbol{\mathcal{K}}$ is the $K \times 1$ observer gain vector

$\hat{x}(n) = \boldsymbol{C}_{\mathrm{prd}}\hat{\boldsymbol{w}}_{\mathrm{prc}}(n-1)$ is the predicted input

$x(n)$ is the observer input, with $x(n) = y_{\mathrm{prc}}(n)$. (5b)

In the above definitions, q is the delay parameter (an integer, in samples) and $\boldsymbol{G}_{\mathrm{sig}}(q)$ is a signal state-transition matrix, for a time-step of $-qT_s$ seconds, i.e.

$$\boldsymbol{G}_{\mathrm{sig}}(q) = \boldsymbol{\Phi}_{\mathrm{sig}}(t)\big|_{t=-qT_s} = \{\boldsymbol{G}_{\mathrm{sig}}^{-1}\}^q = \boldsymbol{G}_{\mathrm{sig}}^{-q}\,. \quad (6)$$

Note that $\boldsymbol{C}_{\mathrm{prd}}$ (for $\hat{x}$) involves the signal and noise subspaces, whereas $\boldsymbol{C}_{\mathrm{obs}}$ (for y_{obs}) considers only the signal subspace.

The gain vector $\boldsymbol{\mathcal{K}}$, is found in the usual way, via a coordinate transform, which reduces the process equations to a canonical form for the observable $\langle\boldsymbol{C}_{\mathrm{prd}}, \boldsymbol{G}_{\mathrm{prc}}\rangle$ pair [22]. The transform required is readily found using the observability matrices of both coordinate systems; alternatively, the discrete-time versions of the Ackermann or the Bass-Gura formulae may be used to find the gain vector directly [21],[22].

The elements of the gain vector $\boldsymbol{\mathcal{K}}$ are chosen to arbitrarily place the poles of the observer in the complex z-plane for the desired convergence characteristics. Let the kth pole of the observer be λ_k (for $0 \le k < K$). All poles must be placed in a way that results in a stable feedback observer (i.e. $|\lambda_k| < 1$). It is also desirable to have a system that is not too oscillatory (i.e. $\angle\lambda_k \approx 0$), with a rate of decay that is slow enough to attenuate white noise (i.e. $|\lambda_k| \to 1$), yet fast enough to quickly remove bias arising from discontinuities in the signal state and from system modelling errors (i.e. $|\lambda_k| \to 0$). Repeated real poles, i.e. $\lambda_k = p$, for all k, with $0 \le p < 1$, are sufficient for low-frequency signals with a narrow bandwidth, or for signals that are sampled at a sufficiently high rate, and they are used exclusively here. However, complex pairs of poles may be required in very-wideband filters. Using $p = 0$ yields a so-called "deadbeat" observer, with an FIR. For a complex argument (arg), |arg| and ∠arg are the magnitude and angle operators, respectively.

F. Filter design

The state observer accepts a scalar-valued input $x(n)$, and produces a vector-valued output $\boldsymbol{w}_{\text{obs}}(n)$. In prediction, filtering, and smoothing, problems (using $q < 0, q = 0$ and $q > 0$, respectively), the position element ($k = 0$) of the state, is of primary importance. To analyze the response of this single-input/single-output (SISO) system, and to yield a minimal-complexity realization of the discrete-time transfer function $\mathcal{H}(z)$, which links the position measurement inputs to the position estimate outputs $y(n)$, it is convenient to determine a new coordinate transform that reduces (5) to a canonical form [21],[22]. The $\boldsymbol{b}$ and $\boldsymbol{a}$ coefficients of the canonical filter realization of $\mathcal{H}(z)$, where $\mathcal{H}(z) = \mathcal{B}(z)/\mathcal{A}(z)$ and $\mathcal{A}(z) = (z-p)^K$, are then readily extracted from the observer equations in canonical form, such that

$$y(n) = \textstyle\sum_{k=0}^{K-1} \boldsymbol{b}(k)x(n-k) - \sum_{k=1}^{K} \boldsymbol{a}(k)y(n-k). \qquad (7)$$

G. Tracker analysis

Bespoke closed-form expressions for the white-noise gain (WNG) of $\alpha-\beta(-\gamma)$ filters are available for various filter configurations [5]-[11]; however, for general cases (i.e. arbitrary order and lead/lag configurations), it may be simply evaluated for any stable transfer function $\mathcal{H}(z)$, using its frequency-response $H(\omega)$, or more conveniently (via a loop until convergence) using its impulse response $h(n)$, as a consequence of Parseval's theorem [26], i.e.

$$WNG = \tfrac{1}{2\pi}\int_{-\pi}^{+\pi} |H(\omega)|^2 d\omega = \tfrac{1}{2\pi}\|H(\omega)\|_2^2$$
$$= \textstyle\sum_{n=0}^{\infty} |h(n)|^2 = \|h(n)\|_2^2 \qquad (8)$$

where $\|\cdot\|_2$ is the $\mathcal{L}_2$-norm. The gain of the maneuver error signal (MESG) is an analogous and complementary narrow-band metric:

$$\text{MESG} = |H_d(\omega_{\text{man}}) - H(\omega_{\text{man}})|^2 \qquad (9)$$

where $\omega_{\text{man}} = \pm\Omega T_s$ or any other frequency of interest in the passband. Now let σ_{tgt}^2 and σ_{man}^2 be the expected squared-distance errors at SS in a Cartesian space with two position coordinates $(\bar{x}, \bar{y})$ – i.e. $\sigma_{\text{sig}}^2 = \langle \varepsilon_{\bar{x}}^2 + \varepsilon_{\bar{y}}^2 \rangle$, where $\langle\cdot\rangle$ is the expectation operator and where bar accents are used to distinguish these coordinate variables from the input and output variables – for a signal produced by the target process model and a target executing a sustained constant-g turn, respectively. Furthermore, assume that white measurement-noise is added with a variance of σ_{sns}^2 in the former case. Then

$$\sigma_{\text{tgt}}^2 = 2\text{WNG} \cdot \sigma_{\text{sns}}^2 \text{ and } \sigma_{\text{man}}^2 = \text{MESG} \cdot R^2. \qquad (10)$$

Note that for an SS-KF with $K = 3$ and $q = -1$: WNG above is the same as ρ_p^2 in (18) of [11] and σ_{man} above is the same as e in (24) of [11]. The maneuver error has components

$$\varepsilon_R = \{|H(\omega_{\text{man}})| - |H_d(\omega_{\text{man}})|\}R \text{ and} \qquad (11a)$$

$$\varepsilon_\theta = \angle H(\omega_{\text{man}}) - \angle H_d(\omega_{\text{man}}) \qquad (11b)$$

where orbital parameters ε_R and ε_θ are the radial and angular errors on the circular trajectory at SS. Note that the metrics in (9)-(11) all consider the desired response H_d, which incorporates, and compensates for, the filter lag induced by q.

The maneuver model may cause the magnitude response of the filter to "bulge" at nearby frequencies. The resulting maxima, typically near dc, in the passband or at the passband edge, may be excited by white noise, which results in low-frequency oscillation or track "wobble". The WNG and MESG metrics are used to quantify the expected squared-distance error; however, the location $\omega_{\max}$, and magnitude of the maximum, i.e. $\|H(\omega)\|_\infty^2$, are an indication of the "color" and severity of the residual errors at SS, where $\|\cdot\|_\infty$ is the $\mathcal{L}_\infty$-norm.

III. Discussion

A. Simulation and parameterization

Monte Carlo (MC) simulations were conducted to investigate and illustrate the behavior of the proposed filters; see Table I for parameterizations A, B & C. The results of an MC instantiation are provided in Fig. 1.

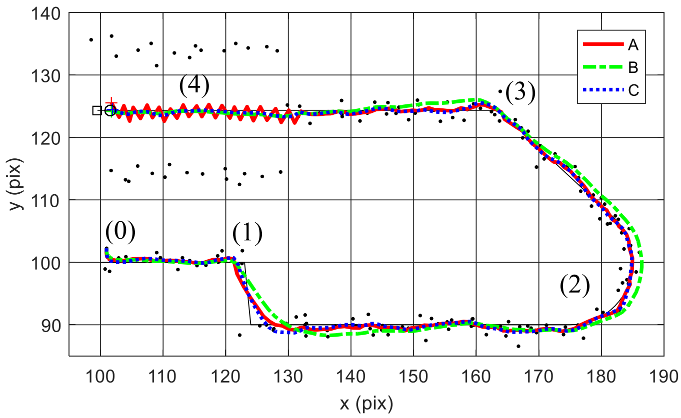

Fig. 1. An MC simulation instantiation showing: True target track, in pixel coordinates (black line); Final target position (black square); Final target position delayed q by frames (black circle); Noisy target measurements (black dots); Track estimates (colored lines). See text for description of scenario events (numbered).

This scenario features the following events: **0)** At frame (frm) index $n = 0$, the track is initiated; **1)** At $n = 24$, the target's apparent $\bar{y}$ position is displaced by 10 measurement cells or pixels (pix), i.e. a position-state discontinuity, e.g. due to a coordinate-registration update; **2)** From $n = 75$ to $n = 99$, it executes a maneuver, with turn radius of $R = 10$ pix and a turn-rate of $\Omega = 2.5$ rad/s; **3)** At $n = 125$, it abruptly changes heading, i.e. a velocity-state discontinuity; **4)** From $n = 160$ to $n = 189$, its apparent $\bar{y}$ position is displaced by ± 10 pix on alternating frames, e.g. "jitter", while the track is updated by two misaligned sensors. It maintains a constant speed throughout, of $v = 25$ pix/s = 1 pix/frm @25 Hz, where $T_s = 0.04$ s. Gaussian measurement noise, with a mean of zero and a standard deviation of $\sigma_R = 1$ pix is added to the target position in each frame.

The KF was tuned using prior knowledge of the simulation parameters (σ_R, Ω & R, see Table I). A variable-gain KF was also implemented. The squared target speed was used to initialize the rate elements of the covariance matrix. The increased initial gain of this filter helped to quickly remove bias errors during track establishment. As no other prior information is supplied on-the-fly, the position element of the Kalman gain vector converges to within 0.1% of the steady-state value (of 0.36) after just 15 updates (i.e. 0.6 s). Events 1, 3 & 4 are the only instances of KF model mismatch in this scenario.

TABLE I: FILTER PARAMETERS*

Filter A†: $K = 2, q = 2$, with $\alpha = 0.36$ and $\beta = 0.08$ in $\boldsymbol{b} = [\alpha - \beta q, \quad \beta(1+q) - \alpha, \quad 0]$ and $\boldsymbol{a} = [1, \quad \alpha + \beta - 2, \quad 1 - \alpha]$
Filter B‡: $K = 3$, $K_{\mathrm{tgt}} = 2, K_{\mathrm{man}} = 0, K_{\mathrm{int}} = 1, q = 2$ with $\boldsymbol{b} = [0.046 \quad 0.004 \quad -0.042 \quad 0]$ and $\boldsymbol{a} = [1 \quad -2.4 \quad 1.92 \quad -0.512]$
Filter C‡: $K = 5$, $K_{\mathrm{tgt}} = 2, K_{\mathrm{man}} = 1, K_{\mathrm{int}} = 1, q = 2$ with $\boldsymbol{b} = [0.0899 \quad -0.1532 \quad -0.0232 \quad 0.1534 \quad -0.0666 \quad 0]$ and $\boldsymbol{a} = [1 \quad -4.0 \quad 6.4 \quad -5.12 \quad 2.048 \quad -0.3277]$

*Independent filters designed for each spatial dimension.

†A 2nd-order SS-KF. This reference implementation was tuned using $\sigma_R = 1.0$ pix and $\sigma_Q = R\Omega^2 = 62.5$ pix/s², respectively.

‡Designed with $\boldsymbol{a}$ extracted from $\mathcal{A}(z)$. Same pole radius as the SS-KF (i.e. $p = 0.8$), to facilitate comparison.

B. Response analysis

The frequency response of the tracking filters is provided in Fig. 2 below.

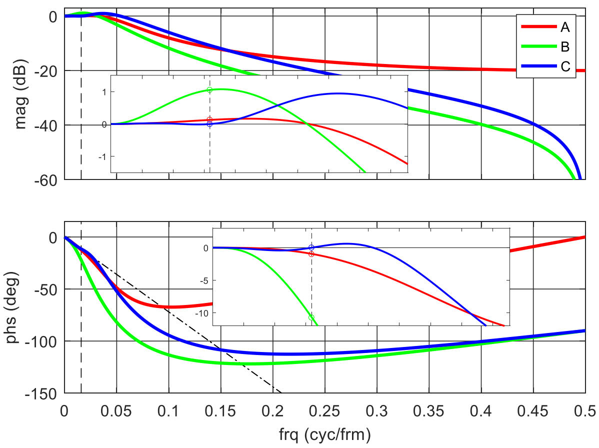

Fig. 2. Filter frequency response, as a function of $f = \omega/2\pi$ (cycles per frame). Maneuver frequency ($f_{\mathrm{man}} = T_s\Omega/2\pi$) and ideal passband linear-phase response (for $q = 2$) shown (dash-dot line). Insets show the low frequency (magnitude and phase-error) response around f_{man} (dashed line).

Prior knowledge of σ_R & σ_Q in **Filter A** (the SS-KF) sets its bandwidth so that the response is approximately flat up to and around the maneuver frequency. The gain and phase error are small at f_{man}. Equation (11) indicates that the SS tracking error for a circular turn of this frequency should also be small, which is indeed the case (see event 2 in Fig. 1). The filter gain rolls off slowly outside the passband (WNG = 0.156) and at $f = 0.5$ the gain is -20 dB or a factor of 0.1 on a linear scale. This indicates that the SS error during the jitter event, with an input magnitude of 10 pix should be approximately ± 1 pix, which is indeed the case (see event 4 in Figure 1).

Use of the interference model in **Filter B** places a null at $f = 0.5$; therefore, the SS error should be zero during the jitter event, in the absence of white noise. This severe high-frequency cut reduces the overall noise gain (WNG = 0.125), but it distorts the response at low frequencies around f_{man}. The negative phase error indicates that the track lags behind ($\sim 11°$) the target executing a circular maneuver at a constant turn rate of f_{man}, at SS. The positive gain of approximately 1 dB at ω_{man} indicates that the track radius is larger than the target radius, at SS. Using $R = 10$ pix, $H(\omega_{\mathrm{man}}) = 1.122$ & $H_d(\omega_{\mathrm{man}}) = 1.0$ in (11a) yields a radial error of $\varepsilon_R = 1.22$ pix at SS, in the absence of noise, which agrees with the overshoot for event 2 in Fig. 1.

The low-frequency distortion caused by the interference model is removed by the introduction of the maneuver model in **Filter C**. In the absence of noise, this model eliminates SS bias errors for turns at the model frequency, and it flattens the response around f_{man}, but it shifts the gain "bulge" to higher frequencies (and increases the noise gain, WNG = 0.188). At those frequencies, this distortion corresponds to: an increase in the SS bias errors (i.e. a leading track with a larger radius) for mismatched circular maneuvers; and an increase in the colored-noise gain (i.e. "wobble"), in the absence of circular maneuvers.

Up to a point, almost all aspects of a tracking filter's performance are improved by increasing q. These gains are of course made at the expense of the system's latency; indeed, it is reasonable to expect greater accuracy if estimates are deferred. Introducing a delay of q samples results in a modulation of the response by $e^{-iq\omega}$ in the frequency domain; its effect on tracking behavior in the time domain is somewhat subtler but readily quantified and appreciated using the material presented in Section II.G.

The complex frequency response is a complete representation of a tracking filter's steady-state behaviour: Integrating the squared magnitude over a band of interest yields its response to random noise inputs, in the absence of manoeuvres; Evaluating it at a frequency of interest yields its response to deterministic sinusoidal inputs, e.g. due to interference or circular manoeuvres, in the absence of noise. The target process model guarantees flatness at $\omega = 0$ for unbiased estimates of position derivatives; the interference process model ensured zero gain at $\omega = \pi$ for improved high-frequency noise attenuation; and the manoeuvre process model ensures unity magnitude and zero phase-error at $\omega = \omega_{\mathrm{man}}$ for perfect tracking of circular turns at the specified angular rate. Each model constrains the response to the desired (complex) value at the specified frequency, but it also shapes or distorts the response elsewhere, which may improve or degrade overall performance.

In the design of optimal infinite-impulse-response (IIR) filters for digital signal processing applications, the pole radius is typically a free parameter, subject to a stability constraint, thus the effective duration of the impulse response is unconstrained. This is reasonable because the signal parameters of interest are approximately stationary over the timescales considered. However, in target tracking problems this is usually not the case, thus the pole radius is fixed (i.e. placed arbitrarily) in the procedure described here, to ensure that the transient response is satisfactory. Constraints on the frequency response are then satisfied, for reasonable SS behaviour – e.g. accurate kinematic state estimation, high-frequency noise attenuation and circular manoeuvre tracking – by the appropriate placement of filter zeros. In this paper, they are placed indirectly through the selection of physical process models and the observer pole position ($0 \leq p < 1$). In [27] & [28] they are derived from the linear coefficients that combine a set of basis functions in a way that satisfies derivative constraints in the ω-domain while (optionally) minimizing the WNG. Process models and pole placement are used here to derive the filter coefficients, primarily to highlight the relationship between the frequency response and the tracking properties of an estimator.

IV. Conclusion

When the statistical distributions assumed in a Kalman filter are unreasonable (e.g. for targets that execute non-Gaussian maneuvers) the intended adaptive behavior is lost, and it must be empirically tuned for the desired transient and steady-state response. Alternatively, if parametric uncertainty is accepted, and variance priors are ignored, the filter design and implementation is greatly simplified, which allows more detailed process models (e.g. maneuver and interference) to be considered for improved steady-state tracking. Observer poles are then placed to set the effective duration of output transients on input discontinuities.

The relationship between a tracking filter's frequency response and its tracking behavior has been discussed and quantified; furthermore, an *ab-initio* design method that specifically addresses (steady-state and transient) response requirements is described in this paper. The simulation results and analysis indicate that the proposed augmented-state observer provides a simple and intuitive way of balancing the various performance trade-offs associated with the design of fixed-gain tracking filters, that would otherwise be difficult to achieve using a standard SS-KF with a filter order equal to the Newtonian state dimension.

References

[1] D. Simon, Optimal State Estimation: Kalman, H-Infinity, and Nonlinear Approaches [& errata], Wiley-Interscience, New Jersey, 2006

[2] P. R. Kalata, "The Tracking Index: A Generalized Parameter for α-β and α-β-γ Target Trackers", *IEEE Trans. Aerosp. Electron. Syst.*, vol. AES-20, no. 2, pp. 174-182, Mar. 1984.

[3] D. F. Crouse, "A General Solution to Optimal Fixed-Gain ($\alpha - \beta - \gamma$ etc.) Filters", *IEEE Signal Process. Lett.*, vol. 22, no. 7, pp. 901-904, Jul. 2015.

[4] J. E. Gray and W. Murray, "The response of the transfer function of an alpha-beta filter to various measurement models", in Proc. *23rd SE Symposium on System Theory*, Columbia, SC, pp. 389-393, 1991.

[5] T. Benedict and G. Bordner, "Synthesis of an optimal set of radar track-while-scan smoothing equations", *IRE Trans. Automatic Control*, vol. 7, no. 4, pp. 27-32, Jul. 1962.

[6] K. Saho and M. Masugi, "Automatic Parameter Setting Method for an Accurate Kalman Filter Tracker Using an Analytical Steady-State Performance Index", *IEEE Access*, vol. 3, pp. 1919-1930, 2015.

[7] J. E. Gray and G. J. Foster, "Filter coefficient selection using design criteria", in Proc. *Twenty-Eighth Southeastern Symposium on System Theory*, Baton Rouge, LA, pp. 275-279, 1996.

[8] J. E. Gray, A. S. Smith-Carroll and W. J. Murray, "What do filter coefficient relationships mean?", in Proc. *Thirty-Sixth Southeastern Symposium on System Theory*, pp. 36-40, 2004.

[9] B. Ekstrand, "Some Aspects on Filter Design for Target Tracking", *J. Control Sci. Eng.*, Article ID 870890, 15 pages, 2012.

[10] B. Ekstrand, "Steady-state circular errors for basic tracking filters", *IEE Proc. - Control Theory and Appl.*, vol. 153, no. 4, pp. 413-418, Jul. 2006.

[11] D. Tenne and T. Singh, "Characterizing performance of α-β-γ filters", *IEEE Trans. Aerosp. Electron. Syst.*, vol. 38, no. 3, pp. 1072-1087, Jul. 2002.

[12] V. Jain and W. D. Blair, "Filter Design for Steady-State Tracking of Maneuvering Targets with LFM Waveforms", *IEEE Trans. Aerosp. Electron. Syst.*, vol. 45, no. 2, pp. 765-773, Apr. 2009.

[13] W. D. Blair, "Design of nearly constant velocity filters for radar tracking of maneuvering targets", in Proc. *2012 IEEE Radar Conf.*, Atlanta, GA, pp. 1008-1013, 2012.

[14] C. C. Arcasoy, "The α-β-Γ tracking filter with a noisy jerk as the maneuver model: frequency domain solution", *IEEE Trans. Aerosp. Electron. Syst.*, vol. 32, no. 3, pp. 1170-1174, Jul. 1996.

[15] C. C. Arcasoy and G. Ouyang, "Analytical solution of α-β-Γ tracking filter with a noisy jerk as correlated target maneuver model", *IEEE Trans. Aerosp. Electron. Syst.*, vol. 33, no. 1, pp. 347-353, Jan. 1997.

[16] A. Bryson and D. Johansen, "Linear filtering for time-varying systems using measurements containing colored noise", *IEEE Trans. Autom. Control*, vol. 10, no. 1, pp. 4-10, Jan. 1965.

[17] A. P. Sage and J. L. Melsa, Estimation theory with applications to communications and control, McGraw-Hill, New York, 1971.

[18] J. D. Gibson, B. Koo and S. D. Gray, "Filtering of colored noise for speech enhancement and coding", *IEEE Trans. Signal Process.*, vol. 39, no. 8, pp. 1732-1742, Aug. 1991.

[19] M. Gabrea, "An adaptive Kalman filter for the enhancement of speech signals in colored noise", in Proc. *IEEE Workshop on Applications of Signal Process. to Audio and Acoustics*, pp. 45-48, 2005.

[20] N. Tanabe, T. Furukawa, H. Matsue and S. Tsujii, "Kalman filter for robust noise suppression in white and colored noises", in Proc. *IEEE Int. Symposium on Circuits and Systems*, Seattle, WA, pp. 1172-1175, 2008.

[21] Katsuhiko Ogata, Discrete-Time Control Systems, 2nd Ed., Prentice Hall, New Jersey, 1995.

[22] R. L. Williams II and D. A. Lawrence, Linear State-Space Control Systems, John Wiley & Sons, New Jersey, 2007.

[23] X. Rong Li and V. P. Jilkov, "Survey of maneuvering target tracking. Part I. Dynamic models", *IEEE Trans. Aerosp. Electron. Syst.*, vol. 39, no. 4, pp. 1333-1364, Oct. 2003.

[24] R. A. Singer, "Estimating Optimal Tracking Filter Performance for Manned Maneuvering Targets", *IEEE Trans. Aerosp. Electron. Syst.*, vol. AES-6, no. 4, pp. 473-483, Jul. 1970.

[25] X. Rong Li and V. P. Jilkov, "Survey of maneuvering target tracking. Part V. Multiple-model methods", *IEEE Trans. Aerosp. Electron. Syst.*, vol. 41, no. 4, pp. 1255-1321, Oct. 2005

[26] T. I. Laakso and S. J. Ovaska, "Optimal polynomial predictors with application specific fixed prefilters", in Proc. *IEEE Int. Symposium on Circuits and Systems* (ISCAS), pp. 351-354, vol.1, 3-6 May 1993.

[27] H. L. Kennedy, "Maximally Flat IIR Smoothers with Repeated Poles and a Prescribed Delay", *IEEE Trans. Signal Process.*, vol. 64, no. 19, pp. 4975-4986, Oct. 2016.

[28] H.L. Kennedy, "Optimal design of digital IIR and FIR filters using complex flatness constraints: A unified approach," in Proc. *Int. Conf. Digital Image Computing: Techniques and Applications (DICTA)*, Gold Coast, pp. 1-8, Nov. 2016.